Journal of Marine Systems 83 (2010) 181–191

Contents lists available at ScienceDirect

Journal of Marine Systems

journal homepage: www.elsevier.com/locate/jmarsys

Alexandrium minutum growth controlled by phosphorus An applied model

A. Chapelle [a,*], C. Labry [a], M. Sourisseau [a], C. Lebreton [b], A. Youenou [a], M.P. Crassous [a]

[a] *Ifremer Dyneco Pelagos, BP70, 29280 Plouzané, France*
[b] *GKSS Research Centre Geesthacht, Institute for Coastal Research, Max-Planck-Straße 1, 21502 Geesthacht, Germany*

ARTICLE INFO

Article history:
Received 15 October 2009
Accepted 21 May 2010
Available online 13 August 2010

Keywords:
Toxic algal blooms
Alexandrium
Phosphorus uptake
Models
Competition
Northwest France

ABSTRACT

Toxic algae are a worldwide problem threatening aquaculture, public health and tourism. *Alexandrium*, a toxic dinoflagellate proliferates in Northwest France estuaries (i.e. the Penzé estuary) causing Paralytic Shellfish Poisoning events. Vegetative growth, and in particular the role of nutrient uptake and growth rate, are crucial parameters to understand toxic blooms. With the goal of modelling *in situ Alexandrium* blooms related to environmental parameters, we first try to calibrate a zero-dimensional box model of *Alexandrium* growth. This work focuses on phosphorus nutrition. Our objective is to calibrate *Alexandrium minutum* as well as *Heterocapsa triquetra* (a non-toxic dinoflagellate) growth under different rates of phosphorus supply, other factors being optimal and constant. Laboratory experiments are used to calibrate two growth models and three uptake models for each species. Models are then used to simulate monospecific batch and semi-continuous experiments as well as competition between the two algae (mixed cultures). Results show that the Droop growth model together with linear uptake versus quota can represent most of our observations, although a power law uptake function can more accurately simulate our phosphorus uptake data. We note that such models have limitations in non steady-state situations and cell quotas can depend on a variety of factors, so care must be taken in extrapolating these results beyond the specific conditions studied.

1. Introduction

The worldwide increase in number of toxic algal events threatens regional economies linked to aquaculture and tourism, as well as public health. In France, one of the most problematic organisms is the dinoflagellate *Alexandrium* which contains toxins that give rise to Paralytic Shellfish Poisoning (PSP) (the French monitoring program, Rephy; the Interreg IIIB NWE Final project; Cembella, 1998). Should these toxic algae be present in areas of aquaculture, the shellfish can, without being harmed, accumulate and concentrate the toxins produced by phytoplankton within their tissues. The ingestion of these contaminated shellfish by humans may lead to serious and potentially fatal gastrointestinal and neurological disorders.

Blooms of *Alexandrium* and PSP events in France date back to the late 1980s (Belin, 1993; Erard-Le Denn, 1997; Probert, 1999). The causative species is *Alexandrium minutum* (Halim). The first cases of toxicity occurred in 1989 in the Bay of Morlaix and in 1992 in the Penzé estuary, which are located in Brittany. Toxic events appeared in 1992, 1993, 1994, 1995, 1996, 1997, 1999 and 2001 (Chapelle et al., 2008) and correspond to *A. minutum* blooms up to 1 million cells L^{-1}. As nitrogen concentration in the Penzé estuary is high and the N/P molar ratio is above 100, nitrogen never limits primary production. On the contrary, phosphate may be limiting and may be controlled by river inputs and sedimentary fluxes which are extremely variable (Andrieux-Loyer et al., 2008). *A. minutum* blooms do not exceed 10 days and may appear from May to July. They are practically never monospecific and not necessarily dominant in terms of phytoplankton biomass. Although *A. minutum* reached 97% of biomass in 1997, its abundance usually remains between 28% and 72% in the other years. In the Penzé estuary, *Heterocapsa triquetra*, a non-toxic dinoflagellate, is frequently associated with *A. minutum* and may be a potential competitor, reaching high concentrations, up to 1 million cells L^{-1} (Labry et al., 2008; Maguer et al., 2004; Morin et al., 2000).

To understand which environmental factors may favour *A. minutum* blooms, numerical modelling associated with *in situ* and laboratory data is often used. Environmental models generally simulate the physical environment based on hydrodynamic models. Coupled to the *Alexandrium* model, these models give good results in terms of knowledge of the relative influence of physical transport, growth or germination on *Alexandrium* blooms (Anderson et al., 2005; Basterretxea et al., 2007; Fauchot et al., 2008; McGillicuddy et al., 2005; Yamamoto et al., 2002; Yamamoto and Seike, 2003). However, the most enduring question remains unknown: why does one specific species — in our case *A. minutum* — bloom in a particular place at a particular time from amongst a diverse phytoplankton population? The relative competitive success of a particular phytoplankton in

* Corresponding author. Tel.: +33 2 98 22 43 56; fax: +33 2 98 22 45 48.
E-mail address: annie.chapelle@ifremer.fr (A. Chapelle).

0924-7963/$ – see front matter © 2010 Elsevier B.V. All rights reserved.
doi:10.1016/j.jmarsys.2010.05.012

different growth conditions is at the root of this question. To answer this question, it is necessary to explore in depth the physiological responses of *A. minutum* linked to environmental parameters. But a compromise should be reached between increasing complexity, requiring kinetics and parameter knowledge, and simpler approaches which are more generic and user-friendly when included in environmental models (e.g., Davidson and Gurney, 1999; Blauw et al., 2010-this issue).

Analysis of *A. minutum* blooms in the Penzé has shown that phosphorus, temperature and residence time are the main factors controlling *A. minutum* blooms, with light being less important and nitrogen being in excess in this ecosystem (Chapelle et al., 2008). As a first step toward building a model of *A. minutum* bloom dynamics, we develop a physiological model of *A. minutum* growth controlled by phosphorus. The model is calibrated and validated with *A. minutum* batch and semi-continuous monospecific cultures. A similar model is built for *H. triquetra* with the same data set. Both models are then applied to simulate the *H. triquetra–A. minutum* competition. The accuracy of the model results is then discussed in relation to model complexity. The next step would then be to incorporate this calibrated growth model in a more general ecosystem model.

2. Materials and methods

2.1. Laboratory experiments and subsequent analyses

The data set is based on cell culture experiments performed on non axenic strains of *A. minutum* (AM89BM) and *H. triquetra* (HT99PZ) isolated in northern Brittany (France) from the Morlaix estuary in 1989 and the Penzé estuary in 1999, respectively. Both strains were maintained in a prefiltered natural seawater enriched f/2 medium (Guillard and Ryther, 1962). For all experiments, cultures were grown at 18 °C, at a salinity of 27, and an overhead illumination of 200 μmol $m^{-2} s^{-1}$ in a 14:10 light/dark (L:D) cycle. Inorganic nitrogen was in excess.

2.1.1. Data set for calibration

To calibrate the *A. minutum* and *H. triquetra* phosphorus models, semi-continuous experiments were carried out along a P limitation gradient using different dilution rates and the same P limited renewal medium (f/2/4 for PO_4, i.e. 8 mmol m^{-3} and f/2 for NO_3, i.e. 880 mmol m^{-3}; Labry et al., 2004). Cells were preconditioned in batch culture then subjected to a semi-continuous mode in duplicate with dilution rates ranging from 0.05 d^{-1} to a maximum of 0.5 d^{-1} for *A. minutum* and 0.6 d^{-1} for *H. triquetra*. After each renewal, the withdrawn water samples were used to measure PO_4, NO_3, and algal cell concentrations. After 10 days of semi-continuous conditions, equilibrium was presumed as changes over 3 days in nutrient concentrations and cell density were less than 10% and 20% respectively in all cultures. On days 1, 2 and 3 after equilibrium, maximal PO_4 uptake rate (V_{Pmax}), P and C internal quotas (P per cell and C per cell) were measured for each dilution rate in addition to PO_4 and algal cell concentrations. For some dilution rates (0.05, 0.1 and 0.2 d^{-1}), half-saturation constants for PO_4 uptake (K_P) were estimated at equilibrium. In this type of culture, at equilibrium, the growth rate (μ) reaches a theoretical value linked to the dilution rate (D): $\mu = -\mathrm{Ln}(1-D)$ (Tilman and Kilham, 1976).

2.1.2. Data set for validation

Validation of *A. minutum* and *H. triquetra* models was performed with various experiments.

Monospecific and mixed batch cultures were conducted to test the response of *A. minutum* and *H. triquetra* cultivated in a PO_4 depleted medium (220 mmol m^{-3} for NO_3). After 1, 2, 3, 5, 7 or 10 days of depletion, a subsample was removed and was subjected to a 4 mmol m^{-3} PO_4 supply (KH_2PO_4, see Labry et al., 2008).

Semi-continuous cultures were achieved with a mean dilution rate of 0.15 d^{-1} (Labry et al., 2008) to test four frequencies (every 1, 2, 4 or 6 days) of PO_4 supply. The PO_4 concentrations in the input medium were 9, 18, 36, and 54 mmol m^{-3} for the frequencies ranging from 1–6 days, respectively. NO_3 was in excess, i.e. 880 mmol m^{-3}. This was performed for *A. minutum* and *H. triquetra* monospecific and mixed cultures.

For all of these experiments, *A. minutum* and *H. triquetra* cell density, PO_4 concentrations and internal P and C cell quota were measured. Cell PO_4 uptake rate data were derived from the difference in PO_4 concentrations between successive days divided by mean cell concentration.

2.1.3. Analyses

For cell enumerations, samples were fixed with a few drops of Lugol's iodine and cells were counted with an inversed optical microscope (Utermöhl method). Samples for PO_4 determination were very carefully filtered on glass fiber filters (Whatman GF/F) with a syringe filtration system. PO_4 was analysed on an autoanalyser AACE Bran and Lubbe following Aminot and Kérouel (2007). Samples for particulate P and C were filtered on precombusted (12 h at 400 °C) 25 mm Whatman GF/D filters (>2.7 μm) and filters were deep frozen (−20 °C). Particulate C was analysed on a CN VarioEL III Elementar analyser after carbonate removal (Aminot and Kérouel, 2004). Particulate phosphorus was determined using a high temperature method (Solorzano and Sharp, 1980). P and C cell quotas (Q_P and Q_C) were obtained by dividing particulate P and C by the corresponding cell number taking into account filtered volumes.

In semi-continuous cultures used for calibration, maximal rates of PO_4 uptake (V_{Pmax}) were measured for each dilution rate at equilibrium using the $^{33}PO_4$ incorporation technique (Jauzein et al., in press). After adjusting the PO_4 concentration of water samples to 10 mmol m^{-3}, incubations started with the addition of 20 μCi $^{33}PO_4$ ($740 \cdot 10^3$ Bq) and were ended by the addition of 4% formaldehyde final concentration. Different incubation times ranging from 5 min to 6 h were tested, and PO_4 uptake rates were calculated on the linear part of the ^{33}P incorporation time series. Half-saturation constants (K_P) were estimated for some dilution rates (0.05, 0.1 and 0.2 d^{-1}) at equilibrium. Incubations were performed by adding various PO_4 concentrations (0.05, 0.1, 0.2, 0.4, 0.8, 1.6, 3.2 and 6.4 mmol $m^{-3} \cdot KH_2PO_4$) and 10 μCi $^{33}PO_4$ ($370 \cdot 10^3$ Bq) to subsamples. At the end of the incubations, samples were filtered on 8 μm Millipore filters. Then, the filters were stored with 4 ml of scintillation cocktail until they were counted with a liquid scintillation counter.

2.2. Building the model

2.2.1. Available models

The Monod (1942) model linking growth directly to extra-cellular nutrient concentrations is one of the most simple models, but it is not adapted to simulate transient growth dynamics related to a non steady-state environment, despite its wide use in 3D ecosystem models (Davidson, 1996; Davidson and Gurney, 1999; Haney and Jackson, 1996; Flynn, 2001; Flynn, 2010; Mitra and Flynn, 2006). Because phosphorus may be accumulated within cells, high growth rates can be maintained for several generations with no or little uptake (Flynn, 2003). In such circumstances, internal cellular quotas become highly relevant. Droop (1973) developed a model linking growth to the internal nutrient pool (or quota). It provides a hyperbolic form of the growth curve using only two parameters, the minimum quota to sustain growth and a maximum theoretical growth rate at infinite quota. Flynn (2002, 2008) proposes a derived Droop function that describes any curve from linear to rectangular hyperbolic using four parameters (maximal growth rate, minimum and maximum quota and an adjustment parameter to set the curve form).

In the Droop model, nutrient uptake is dependent on extra-cellular nutrient concentration but is not linked to the quota. However, experiments have shown that, uptake kinetics is often linked to nutrient status, and only more complex mechanistic models, which consider feedback processes or multiple internal pools are able to accurately reproduce the biochemical reality (Davidson and Gurney, 1999; Flynn, 2003; Flynn, 2008; John and Flynn, 2000).

2.2.2. Model description

To calibrate the *A. minutum* and *H. triquetra* phosphorus models, we used semi-continuous culture data at equilibrium with phosphorus quota calculated by cell (Q_P in pg cell^{-1}) or by C content ($Q_{P/C}$ in mmol P mol C^{-1}). In fact, the Droop model was initially built with quota per cell data but as cell size may vary with nutrient stress, quota per C is probably more reliable (Flynn, 2008). Carbon-based quota and cell quota are equivalent only if cellular carbon content remains constant, which is not the case in these experiments (data not shown). Both relationships are tested here.

2.2.2.1. Growth rate. Data show the relation between growth rate and the quota expressed per cell or per C for *A. minutum* and *H. triquetra* (Fig. 1). It was not possible to evaluate $\mu = f(Q_{P/C})$ with the Droop formulae or with any other relevant formulae because of the unusually high variability of μ as a function of quota (Fig. 1ab). This variability could be explained by cultures being close to washout due to the dilution rate approaching the maximum growth rate of cells. Thus the culture data may not reflect equilibrium. This variability could also suggest time-lag behaviour, with growth not dependent on instantaneous quota (Collos, 1986; Cunnigham and Maas, 1978; Davison et al., 1993; Davidson and Cunningham, 1996; Nyholm, 1978). However, according to these authors the time-lag is in general more obvious for the cell quota than for the C quota, which is not the case here. A third hypothesis is the influence of some other limiting factors not taken into account in these experiments. The culture data for phosphorus quota (Fig. 1cd) are more suitable for parameterization in our model. We therefore proceed with a P cell^{-1} quota model, keeping in mind that for future applications, other factors as temperature, light, etc. could affect cell quotas.

The Droop and Flynn (2002) models were chosen to simulate *A. minutum* and *H. triquetra* growth rate (μ) linked to P quota (Q_P). The Droop model is defined as

$$\mu = \mu_{\max th} \times \left(1 - \frac{Q_{P\min}}{Q_P}\right)$$

where $\mu_{\max th}$ is the theoretical maximum growth rate (at infinite quota), and $Q_{P\min}$ is the minimum Q_P quota below which there is no growth. The Flynn model is

$$\mu = \mu_{\max} \times \left(\frac{(1 + KQ) \times (Q_P - Q_{P\min})}{(Q_P - Q_{P\min}) + KQ} \times (Q_{P\max} - Q_{P\min})\right)$$

where $\mu_{\max}$ is the maximum growth rate (at maximum quota) and $Q_{P\min}$, $Q_{P\max}$ and Q_P are the minimum, the maximum and the phosphorus quota, respectively. KQ is a dimensionless parameter to set the curve form.

2.2.2.2. Nutrient uptake. Nutrient uptake (V_P) is linked to the external nutrient concentration, following the Michaelis–Menten relation:

$$V_P = V_{P\max} \times \frac{PO_4}{(PO_4 + K_P)}$$

where K_P is the half-saturation constant. It was calibrated with the semi-continuous cultures (Labry et al., 2004; Table 1) and corresponds to the measured minimum values (0.28 mmol m^{-3} for *A. minutum* and 0.97 mmol m^{-3} for *H. triquetra*).

V_P and $V_{P\max}$ are expressed in pg cell^{-1} d^{-1} and correspond to the phosphorus uptake rate and to the maximum uptake rate, respectively. $V_{P\max}$ is constant in the Droop formulation, which is not reliable (as discussed previously), nor supported by the data (Fig. 2). Observations by Labry et al. (2004) show that uptake was maximal when the quota was low and decreased as cell quota increased.

The maximal measured value for *A. minutum* was higher than that obtained following Droop ($\mu_{\max th} \times Q_{P\max} = 28$ pgP cell^{-1} d^{-1}), which could reflect surge transport, which is uptake above that required to support maximal growth (Collos, 1983; Flynn et al., 1999). This was not the case for *H. triquetra* whose measured maximal uptake

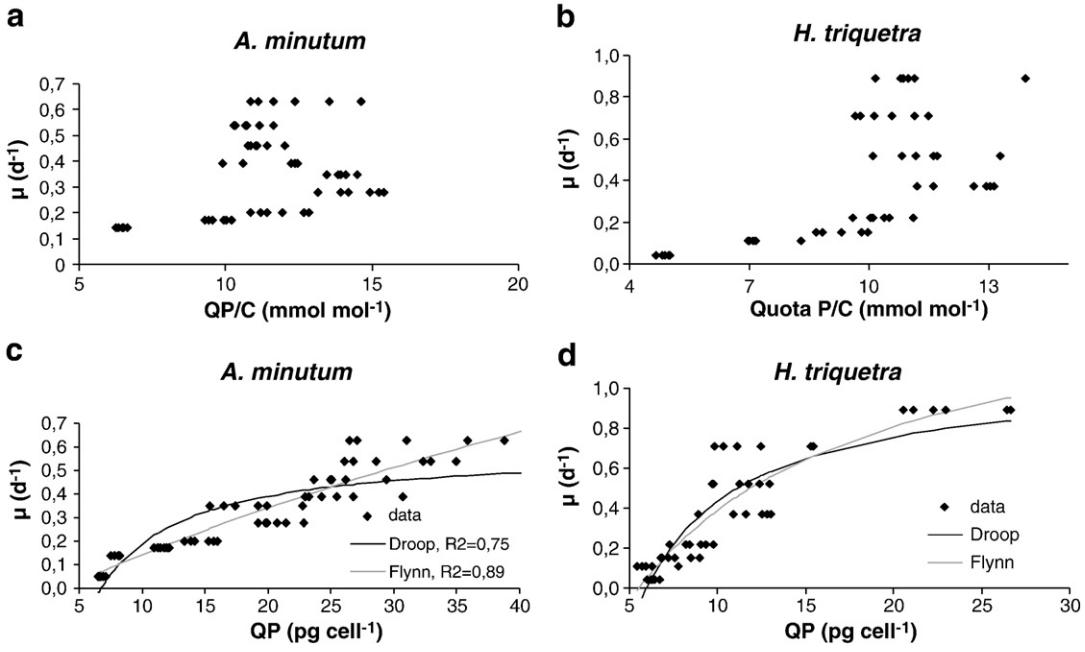

Fig. 1. Growth rate versus P quota for *A. minutum* and *H. triquetra*. a: *A. minutum* growth rate versus $Q_{P/C}$ quota; b: *H. triquetra* growth rate versus $Q_{P/C}$ quota; c: *A. minutum* growth rate versus Q_P quota in cells; and d: *H. triquetra* growth rate versus Q_P quota in cells. Data are provided from semi-continuous experiments at equilibrium (Labry et al., 2004).

Table 1
Parameter set for the model. Am: *Alexandrium minutum*; and Ht: *Heterocapsa triquetra*.

Parameters	Species	Value	Units	References
Maximum measured growth rate at 18 °C (μ_{max})	Am	0.63	d^{-1}	Labry et al. (2004)
	Ht	0.89	d^{-1}	Labry et al. (2004)
Maximum Droop adjusted growth rate (μ_{maxth})	Am	0.59	d^{-1}	This study
	Ht	1.08	d^{-1}	This study
Maximum Flynn adjusted growth rate (μ_{max})	Am	0.55	d^{-1}	This study
	Ht	0.67	d^{-1}	This study
Maximal measured phosphorus cell quota (Q_{Pmax})	Am	48	pg $cell^{-1}$	Probert (1999)
	Ht	23.3	pg $cell^{-1}$	Labry et al (2008)
Minimum measured phosphorus cell quota (Q_{Pmin})	Am	5.9	pg $cell^{-1}$	Bechemin et al (1999)
	Ht	4.1	pg $cell^{-1}$	Labry et al. (2008)
Minimum Droop adjusted phosphorus cell quota (Q_{Pmin})	Am	6.8	pg $cell^{-1}$	This study
	Ht	6.0	pg $cell^{-1}$	This study
Minimum Flynn adjusted phosphorus cell quota (Q_{Pmin})	Am	3.7	pg $cell^{-1}$	This study
	Ht	5.5	pg $cell^{-1}$	This study
Maximum Flynn adjusted phosphorus cell quota (Q_{Pmax})	Am	32.6	pg $cell^{-1}$	This study
	Ht	15.6	pg $cell^{-1}$	This study
Flynn adjusted KQ	Am	4.24	–	This study
	Ht	1.34	–	This study
Half-saturation constant for PO_4 assimilation (measured) (K_P)	Am	0.28–1.62	µmol l^{-1}	Labry et al. (2004)
	Ht	0.97–2.23	µmol l^{-1}	Labry et al. (2004)
Maximum measured PO_4 uptake rate	Am	39.3	pg.$cell^{-1}$ d^{-1}	Labry et al. (2004)
	Ht	24.8	pg.$cell^{-1}$ d^{-1}	Labry et al. (2004)

was nearly the same as the maximum calculated by Droop ($\mu_{maxth} \times Q_{Pmax} = 25$ pgP $cell^{-1}$ d^{-1}).

This type of feedback mechanism is a common feature among phytoplankton species and has been described and modelled for different species and different nutrients (NO_3, NH_4, and PO_4). The form of the curve is dependent on the nutrient, the species, and the representation of the quota (per cell or per C) (see Davidson and Gurney, 1999; Ducobu et al., 1998; Flynn et al., 1999; Geider et al., 1998; Morel, 1987; Riegman et al., 2000; Roelke et al., 1999; Thingstad, 1987).

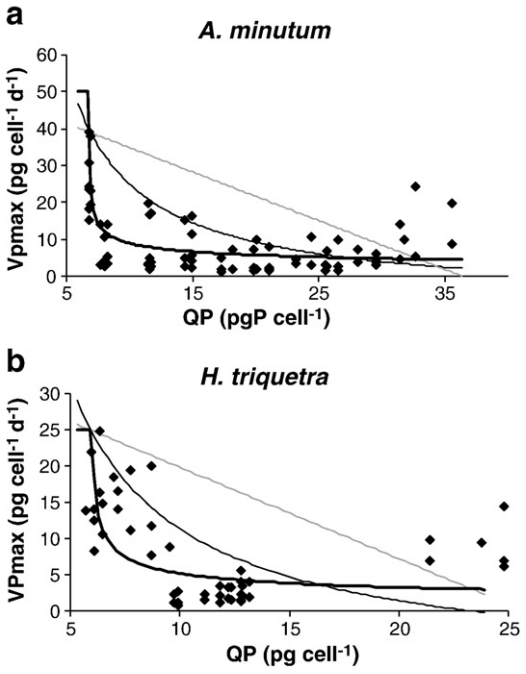

Fig. 2. Maximal phosphorus uptake (V_{Pmax}) versus internal quota (data from Labry et al., 2004). a: *A. minutum* uptake rate versus Q_P quota in cells; and b: *H. triquetra* uptake rate versus Q_P quota in cells. Fine dark line: Hyperbolic uptake; gray line: linear uptake; thick dark line: power law uptake.

Different curve choices can be made to fit the data (Fig. 2). The most important objective is to model the decreasing part of the curve. We note that the V_{Pmax} increase for larger quotas corresponds to longer time incubations which are not as representative of the uptake process (see Labry et al., 2008).

Three functions were tested for *A. minutum* and *H. triquetra*:

- The linear function, described by a slope calculated with the maximal measured uptake for minimal measured quota and the minimum measured uptake for the maximum measured quota: $V_{Pmax} = V_{Pmaxa} - (slope \times (Q_P - Q_{Pmin}))$. V_{Pmaxa} is the absolute measured maximum uptake rate.
- The hyperbolic function: $V_{Pmax} = V_{Pmaxa} \times \frac{\left(1-\frac{Q_{Pmax}}{Q_P}\right)}{\left(1-\frac{Q_{Pmax}}{Q_{Pmin}}\right)}$ enabling increase in the difference between low and high quota compared to the linear relation.
- The power law function: $V_{Pmax} = Min\left(a \times (Q_P - Q_{Pmin})^b; Q_{Pmax}\right)$ which gives a more abrupt response at small quotas, but it does not have mechanistic meaning in this context. For *A. minutum*, a and b are 12.3 and −0.31, respectively. For *H. triquetra*, a and b are 8.8 and −0.38, respectively.

2.2.3. Running the model

The numerical model was written with the Stella 9.1 modelling software system. It is a 0D model built to reproduce algal growth in different phosphorus environments. For all simulations we used the Runge–Kutta 4th order method with a time step of 0.01 day. The simulation time corresponds to the experiment time (15–20 days).

To quantify the agreement between results and data, an agreement index (I) was calculated, which corresponds to the relative variation for each modelled variable compared to data:

$$I = \frac{1}{n}\sqrt{\sum_{i=1}^{n}\left(\frac{simu_i - data_i}{data_i}\right)^2}$$

where $simu_i$ and $data_i$ are the simulated and observed values, and n is the number of data. This agreement index was used to compare kinetics and model results to the data and it is a tool used to select different modelling options. The smaller the agreement index is, the better the fit.

3. Results

3.1. Calibration of the phosphorus model with monospecific culture experiments

3.1.1. Growth and uptake kinetics

Both growth models, Droop and Flynn, were fit to the data using the least method, giving realistic values of μ_{maxth} or μ_{max} and Q_{Pmin} and Q_{Pmax} compared to measurements for *A. minutum* as well as for *H. triquetra* (Fig. 1, Table 1). As for the uptake kinetics, the power law function shows the best fit for both algae (Fig. 2, Table 2). The linear function overestimates the uptake and gives the worst fit. The hyperbolic function gives an intermediate result.

3.1.2. Application on monospecific batch experiments

Kinetics (growth and uptake), with parameters fit to the semi-continuous experiments, were then tested in batch conditions on *A. minutum* and *H. triquetra* monospecific cultures (Labry et al., 2008). All models reproduce algal growth responses to different PO_4 pulses, showing an increase in the cell abundance due to growth, delayed 2–

Table 2
Agreement index for *Alexandrium minutum* and *Heterocapsa triquetra* models. The agreement index (Section 2.2.3) is used to quantify the fit of the different models to data.

Agreement index					
Uptake kinetics	*A. minutum* V_{Pmax}		*H. triquetra* V_{Pmax}		
Hyperbolic uptake	0.44		0.31		
Linear uptake	0.79		0.63		
Power uptake	0.17		0.13		
Monospecific batch cultures					
	A. minutum		*H. triquetra*		
Models	Am	PO_4	Ht	PO_4	
Droop hyperbolic	0.11	3.91	0.18	3.67	
Droop linear	0.08	2.09	0.22	1.24	
Droop power	0.1	5.5	0.17	6.87	
Flynn hyperbolic	0.11	8.81	0.17	6.6	
Flynn linear	0.08	3.74	0.22	1.24	
Flynn power	0.12	7.37	0.17	6.87	
Monospecific semi-continuous cultures					
	A. minutum			*H. triquetra*		
	Am	PO_4	Q_P	Ht	PO_4	Q_P
Droop linear	0.05	0.22	0.12	0.06	0.29	0.15
Droop power	0.07	3.38	0.13	0.09	5.52	0.16

3 days after the pulse (Fig. 3). This lag is due to time required to fill the internal P quota. Levels of *A. minutum* or *H. triquetra* at the end of the experiments are the same for 1, 2, 3 and 5 day pulses but lower for 7 and 10 days. This is because the experiment stopped before the stationary phases. In the model, the same cell abundance value was obtained for all experiments after 15 days simulation.

Droop and Flynn kinetics as calibrated in Section 3.1.1 show comparable performance in simulating algal abundance, yielding similar agreement index values (Table 2). However, the Droop model fits the PO_4 drawdown better for *A. minutum*. With the Flynn growth model, more time is required for PO_4 consumption after the pulse (Fig. 3). Concerning uptake models, the results of the simulations are not obvious: although the linear model was the least adjusted to uptake kinetics, the results for *A. minutum* abundance and PO_4 in both algae provide the best fit. The power model is the best only for describing *H. triquetra* abundance. In fact, the linear model is the best for reproducing the quick drop of PO_4 after the pulse, then the hyperbolic one and finally the power model (Fig. 3).

Although both Droop and Flynn growth models yielded comparable agreement indices in fitting the data in aggregate (Table 2), we chose to proceed with the Droop model because it provided a better fit to the phosphate drawdown data for our primary species of interest, *A. minutum*. In the following section, all three uptake models were simulated with the Droop growth model. For brevity, only the results of the linear model (giving the best fit to monospecific batch model simulations) and of the power model (giving the best agreement with uptake kinetics calibrated on monospecific semi-continuous experiments) will be presented.

3.2. Validation on monospecific semi-continuous experiments

The models are applied to semi-continuous experiments with 0.15 d^{-1} dilution rate and different PO_4 supply frequencies (Figs. 4, 5: only 1 and 6 day intervals are shown). Both models simulated the overall changes in algae abundance, phosphorus quota and phosphate in response to PO_4 pulses. In the beginning of the experiment with 1 day and 2 day (not shown) pulse intervals, cell concentration increased exponentially as in batch culture mode (ignoring the daily water removal signal evident in the simulation). For the 4 day (not shown) and 6 day intervals, we observed an increase in cell abundance after the PO_4 pulse, and then a decrease until the next pulse. Both uptake models gave almost the same result concerning algal abundance, with the same agreement index (Table 2). In contrast, quota and especially PO_4 are better simulated by the linear model. As in the results for the batch culture, the power model was not able to reproduce enough PO_4 consumption after the pulse and PO_4 concentrations were overestimated.

3.3. Application of the A. minutum/H. triquetra competition (batch and semi-continuous experiments)

Models, described previously for *A. minutum* and *H. triquetra*, are combined in this section to simulate competition (mixed cultures).

3.3.1. Semi-continuous mixed culture experiments

In these semi-continuous experimental conditions, *A. minutum* always outgrew *H. triquetra* (Fig. 6). This feature is well reproduced by the linear model. However, the power law model shows correct result of the competition with *A. minutum* abundance greater than *H. triquetra* for a short pulse delay (1 day, 2 days, data not shown) but the same final abundance for both algae in the case of greater pulse delays (4 days and 6 days). This is not realistic.

3.3.2. Batch mixed culture experiments

In simulation of mixed batch culture, both populations reach abundances of approximately the same order as the observations (Fig. 7). The simulations show that the competition issue is dependent on the timing of the pulse. For early pulses (1 day; 2 day pulse not shown) and with the linear uptake, *H. triquetra* is dominant. Competition in the linear model shifts to favour *A. minutum* for a pulse arrival at 5 days, which is consistent with the observations; the power law model is unable to simulate this shift. Both models overestimate *H. triquetra* abundance for the 10 day pulse. The linear model provides a better approximation to the *A. minutum* and phosphate time series than the power law model.

4. Discussion

The models presented here have been used to simulate various data sets: batch, semi-continuous, monospecific cultures and mixed cultures of the 2 algal species, *A. minutum* and *H. triquetra*. This variety of experimental data provides strong constraints for model testing. The results indicate that the linear model provides the best fit. The power law model fails to resolve the competition between *A. minutum* and *H. triquetra* in mixed culture, and gives bad fits for PO_4 in almost every situation. This is a surprising result as the power law model was the best representation of uptake at the calibration stage. We will first discuss the linear model results, followed by those of the power law model.

4.1. Response of A. minutum and H. triquetra in case of P-culture control

The linear model successfully simulates algal growth and PO_4 uptake in the case of batch experiments. *H. triquetra* grows more quickly than *A. minutum* in monospecific experiments and reaches higher abundance at the end of the experiment. The linear model captures this feature but underestimates *H. triquetra* abundance. This is probably due to overestimation of the *H. triquetra* quota in the Droop formulation as compared with the measured quota which is lower (Table 1).

For phosphorus pulsing in monospecific cultures, the later the pulse arrives, the greater the phosphorus depletion. Following P depletion, the modelled P pulse is shortened from 4 days (pulse day 1) to 2 days (pulse day 10) for *A. minutum* and from 4 days to 3 days for *H. triquetra*. This is due to an increase in uptake when P quota is

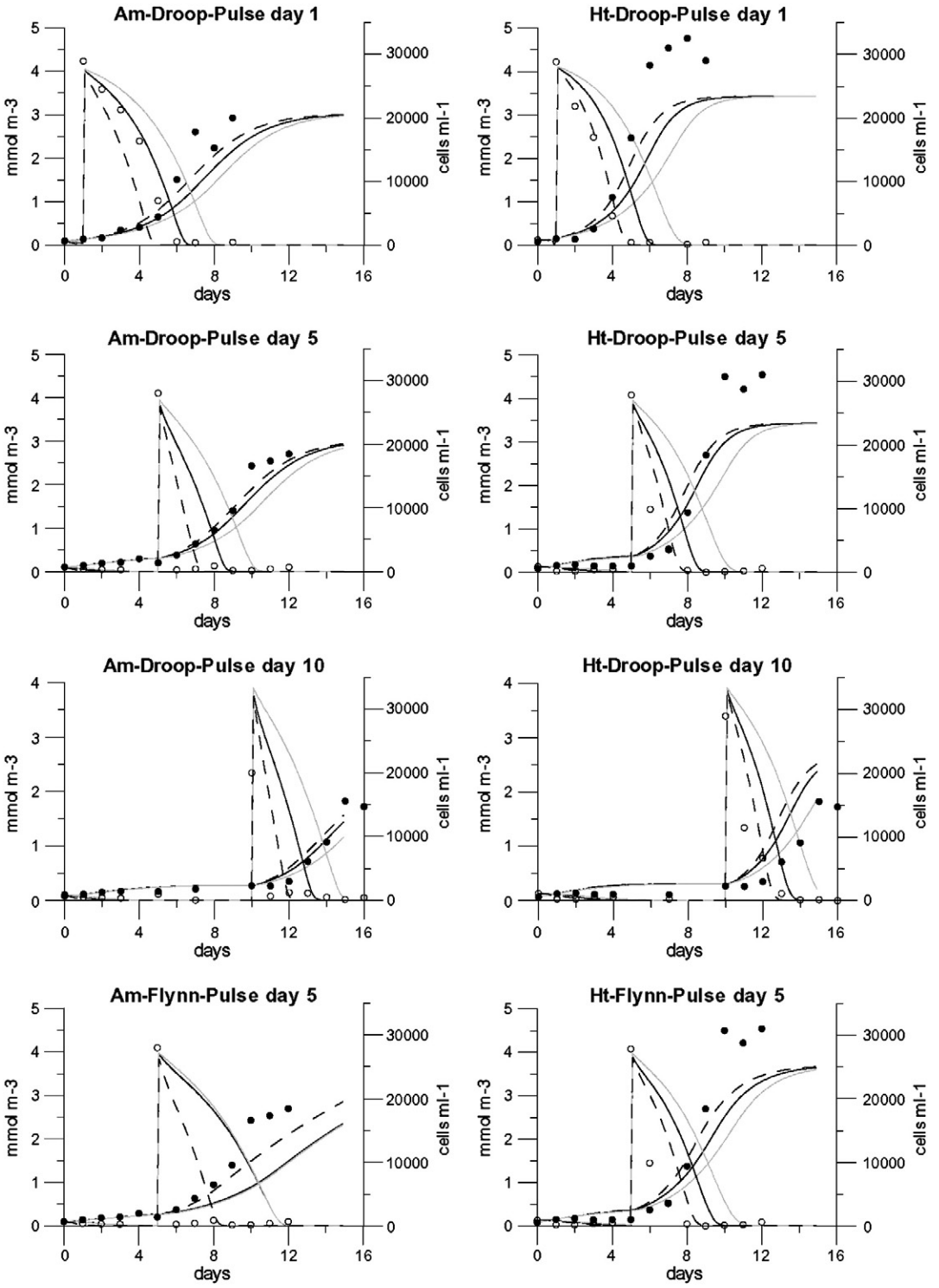

Fig. 3. Application of the model on monospecific batch culture data (●: algal abundance in cells ml^{-1}; O: PO_4 in mmol m^{-3}). Am is for *A. minutum* and Ht is for *H. triquetra*. Droop is for Droop growth description; Flynn is for Flynn growth description. ——: hyperbolic model; —— : power law model; and – – – – : linear model.

lowered (quota simulated but not shown), and the increase is greater for *A. minutum* than for *H. triquetra*. Thus, in the case of high P depletion, the *A. minutum* model reproduces the greater ability of *A. minutum* to take up P. This aspect permits simulation of the observed shift from *H. triquetra* dominance to *A. minutum* dominance after 3 days of P depletion when both algae are cultivated together (Labry et al., 2008). *H. triquetra* is more competitive at high P concentrations due to its higher growth rate; however in the case of P depletion it is outcompeted because *A. minutum* has a better affinity for P uptake at low concentrations. After 10 days of depletion followed by a pulse, the P quota is enhanced threefold for *A. minutum* and only twofold for *H. triquetra* (results simulated but not shown).

Even if the phytoplankton signal and PO_4 pulse are well simulated, the models can have difficulty representing the drop of PO_4 after the pulse, especially in the case of severe P depletion (delayed pulse). The models thus tend to underestimate PO_4 uptake. Possible explanations

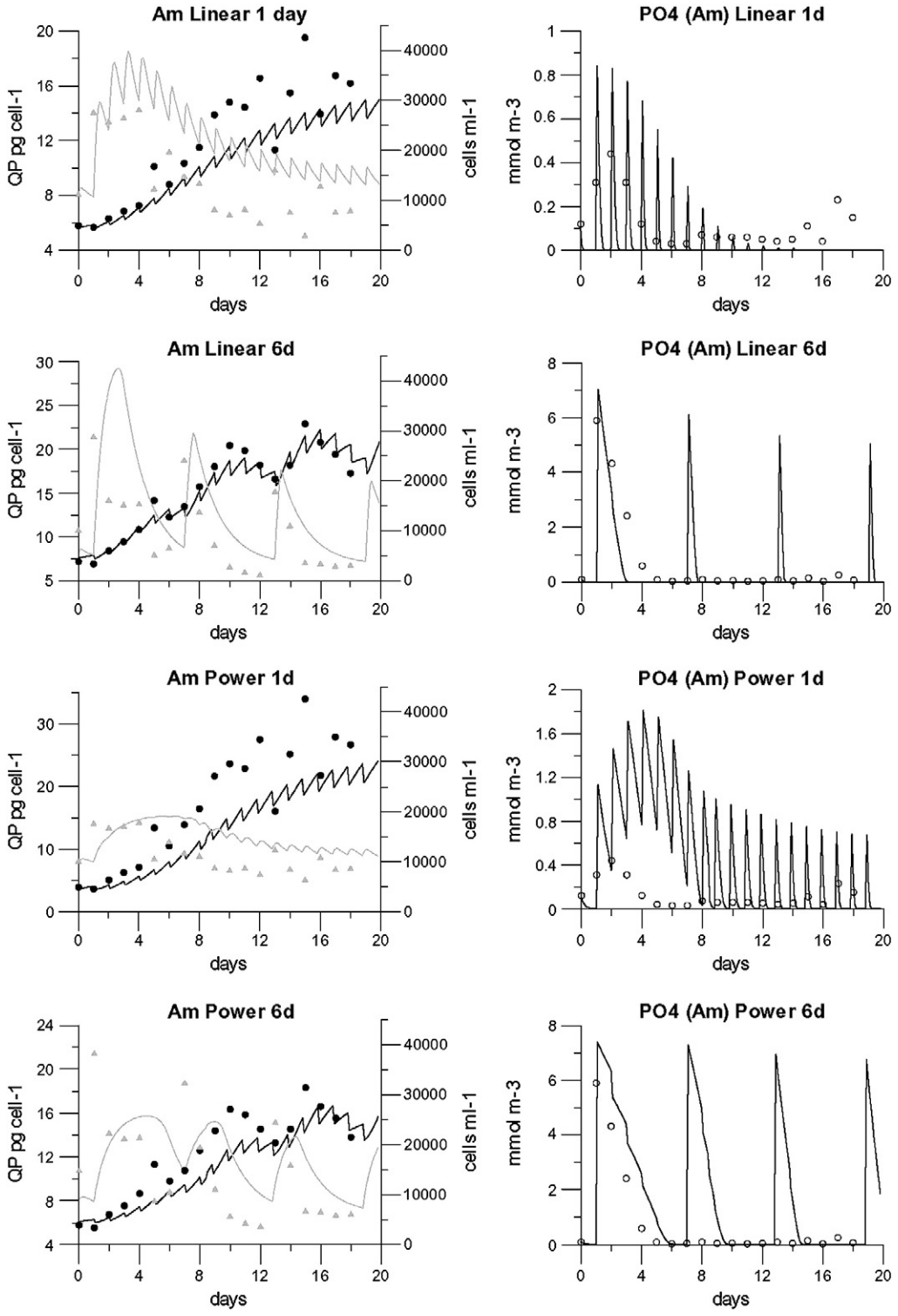

Fig. 4. Simulation of *A. minutum* grown in semi-continuous experiments using two of the four frequencies of PO_4 supply: 1 day and 6 day interval. ––: simulation; ●: *A. minutum* data; ▲: Phosphorus quota data; and O: PO_4 data.

include: underestimation of PO_4 uptake rate data, a time-lag between quota repletion and PO_4 uptake, and non-algal control on PO_4 uptake. More detailed explanation will be provided in the following section.

In semi-continuous monospecific cultures *H. triquetra* reaches higher density than *A. minutum*. The model reproduces this tendency but it underestimates *H. triquetra* abundance due to an overestimation of the P cell quota. *A. minutum* P cell quota shows variations following the P pulse in accordance with data, but the model seems to slightly overestimate the P cell quota. This means that in culture, *A. minutum* is able to have a quicker use of P cell quota than simulated by the linear model.

4.2. Accuracy and predictability of the uptake model

On one hand, the linear model provides better fidelity to the experimental data for many different growth conditions for *A. minutum* as well as competition. On the other hand, the power law

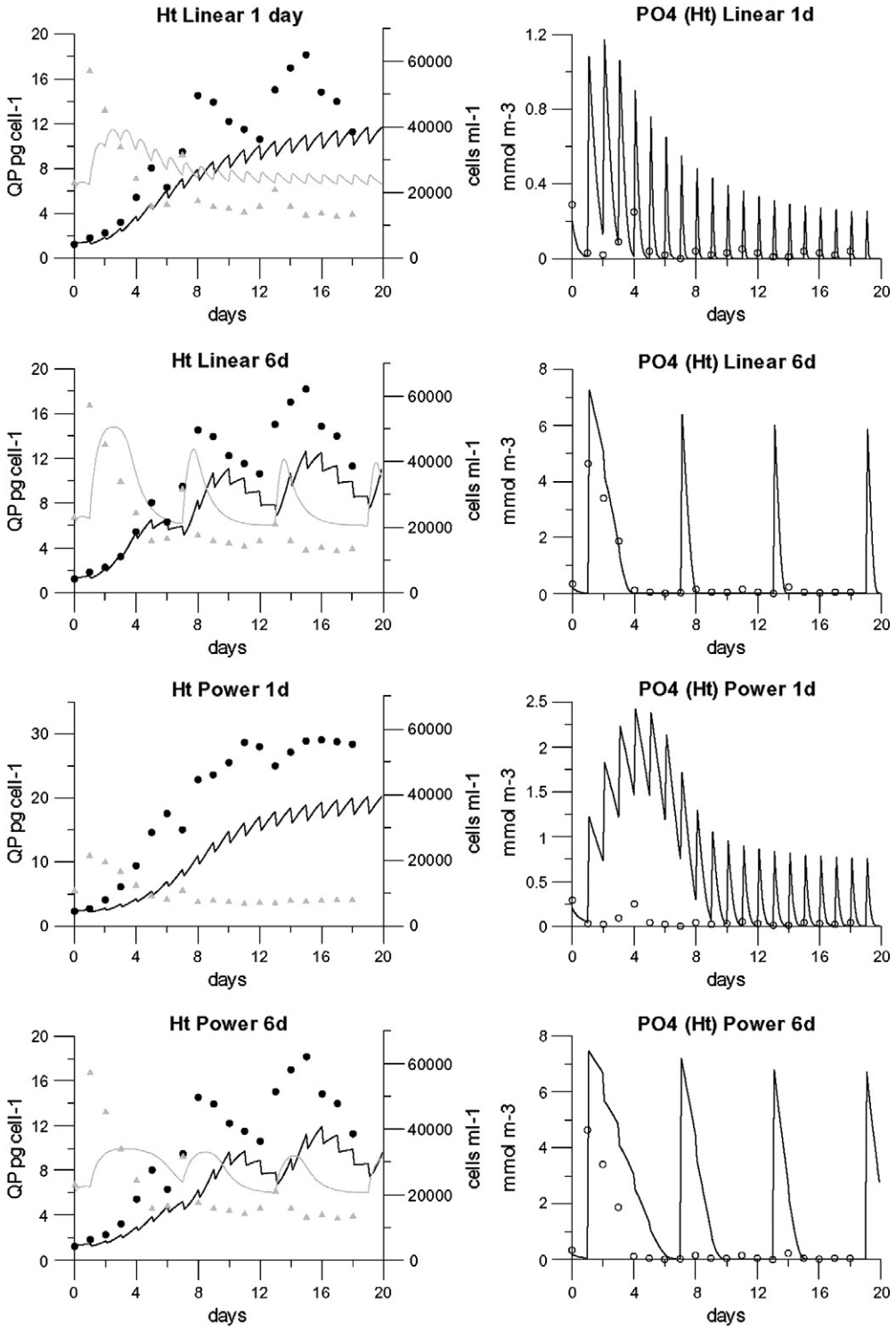

Fig. 5. Simulation of *H. triquetra* grown in semi-continuous experiments using two of the four frequencies of PO_4 supply: 1 day and 6 day intervals. ––: simulation; ●: *H. triquetra* data; ◢◣: Phosphorus quota data; and O: PO_4 data.

model simulates phosphorus uptake kinetics more accurately than the linear model. The question is thus: why does the linear model, which is poorly fitting the uptake measurements, give better results in simulating growth rate experiments?

In semi-continuous experiments (Fig. 1), the linear and the power law curve predict equal uptake for small quotas. For higher quotas, linear fitting gives a larger uptake value.

The nutrient pulses introduced into the cultures are transient events. In the batch experiments, for small P depletion, algal quotas were not minimum when the P pulse occurred. But in the case of severe P depletion (pulse after 5 days), quotas were minimum but increased very quickly, thus reaching the range of quota where the linear model displays a greater uptake than the power law model. Thus, the linear model seems more adapted to simulate transient events.

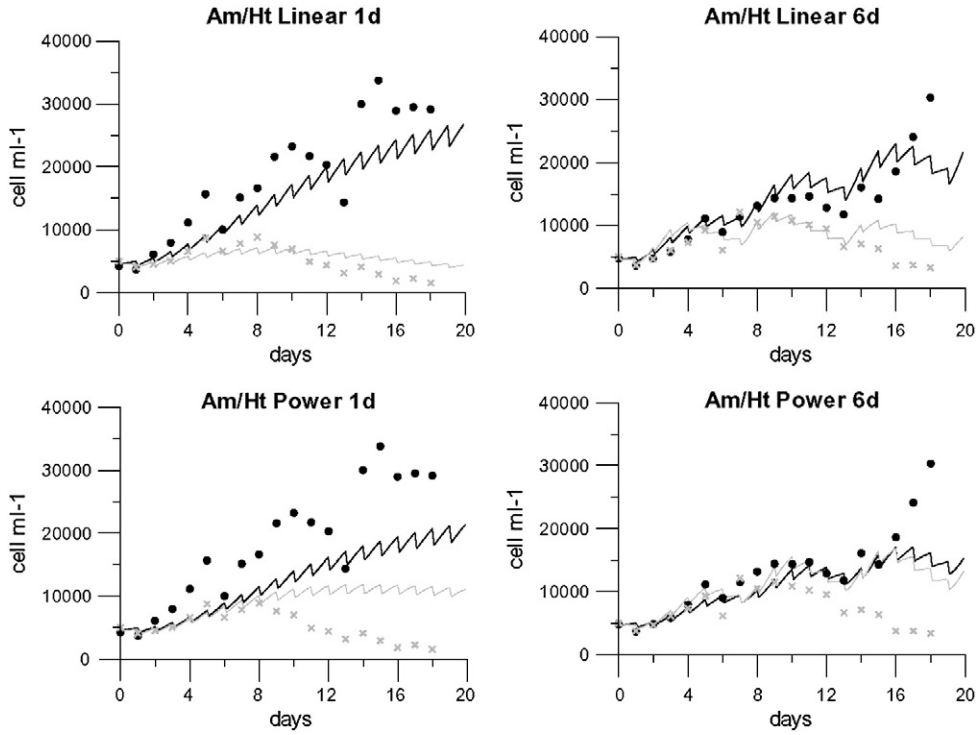

Fig. 6. Simulation of *A. minutum/H. triquetra* competition (mixed cultures) in semi-continuous experiments using two of the four frequencies of PO_4 supply: 1 day and 6 day intervals.–– :*A. minutum* simulation; ●: *A. minutum* data; –– : *H. triquetra* simulation; and ×: *H. triquetra* data.

The next question is: Why is it necessary to simulate a greater uptake than the one fitted by the power law curve to improve the PO_4 concentrations simulated in all batch and semi-continuous experiments?

The first potential explanation lies in an underestimation of phosphate uptake data used for calibration. The uptake measurements (V_{Pmax}) were achieved on semi-continuous cultures at equilibrium and calculated on the linear part of the ^{33}P incorporation time series for incubation time ranges depending on the degree of P limitation cells (between tens of minutes to several hours after the addition of saturating PO_4). These are instantaneous uptake measurements. Sciandra (1991) showed that nitrogen uptake rate changed during 24 h after daily NO_3 additions to cultures of *Prorocentrum minimum* (increase first during several hours followed by a decrease). The same may be true for phosphate uptake, but that aspect was not measured in the 24 h ^{33}P incorporation experiments. Our data may thus underestimate the actual phosphate uptake rate. The best way to measure steady-state phosphate uptake would be in continuous cultures. However, the physiological state of *A. minutum* cells is known to be sensitive to automatic agitation of culture medium (Probert, 1999). We thus chose to manage semi-continuous cultures with gentle stirring once a day only.

The second possible explanation lies in the difference between batch cultures and semi-continuous cultures. Uptake rate data were adjusted against quota measurements in an equilibrium status. In batch experiments, the cells were cultivated under more or less severe P depletion but quickly reacted when a P pulse occurred. The nutrient pulse is a very transient event. Cells may need time to adapt to these new conditions, and even if the quota increases, the uptake may remain at an elevated level because the cells were previously suffering from P deficiency. To simulate this, it would be necessary to include a time-lag with an uptake function of historical internal quota as has been done for time-lag growth (Davison et al., 1993; Davidson and Cunningham, 1996). Alternatively, an intermediate metabolite pool to control the uptake could be adopted, as in Flynn (2003).

The third explanation, which is not in contradiction with the previous ones, could be that phosphate concentration was not solely controlled by algal uptake. PO_4 uptake by bacteria is known to be high in P depleted conditions (Labry et al., 2002) and the competition between algae and bacteria for phosphate could be very complex. Because the cultures were non axenic, measured PO_4 uptake includes not only algal uptake, but also bacterial uptake. Our choice of non axenic cultures was based on the finding that antibiotic treatments may affect the metabolism of algae especially their toxin production (Maas et al., 2007). It is possible to estimate the effect of bacterial uptake on semi-continuous cultures. In these cultures, particulate phosphorus was measured on >2.7 μm particles (GF/D filters) to estimate P algal cell quota. The difference between PO_4 consumption and the increase in P cell quota provides an upper bound on the possible PO_4 bacterial uptake. Computing the mean of this effect for all four pulsing experiments yields 18% of PO_4 consumption for *A. minutum* monospecific cultures and 16% for *H. triquetra* monospecific cultures.

It is also possible that excretion of dissolved organic phosphorus (DOP) by algae could contribute to these apparent discrepancies. Unfortunately DOP was not measured therefore this aspect cannot be addressed. However, DOP excretion does not explain the quick PO_4 decrease after the pulse in the batch cultures.

Considering these various possible explanations, and keeping in mind that the objective here is to develop an *A. minutum* model to be included in an ecosystem model to predict *A. minutum* blooms and PSP risks, we find the Droop growth–linear uptake model to be the most suitable for simulating various experimental conditions. In the future when the model is included in the Penzé ecosystem model, other compartments reacting with PO_4 and *A. minutum* will be added (such as a bacterial compartment, other nutrients, grazers, as well as physical effects).

5. Conclusions

A model of phosphorus uptake and algal growth is proposed for *A. minutum* and *H. triquetra*. This model includes the Droop description

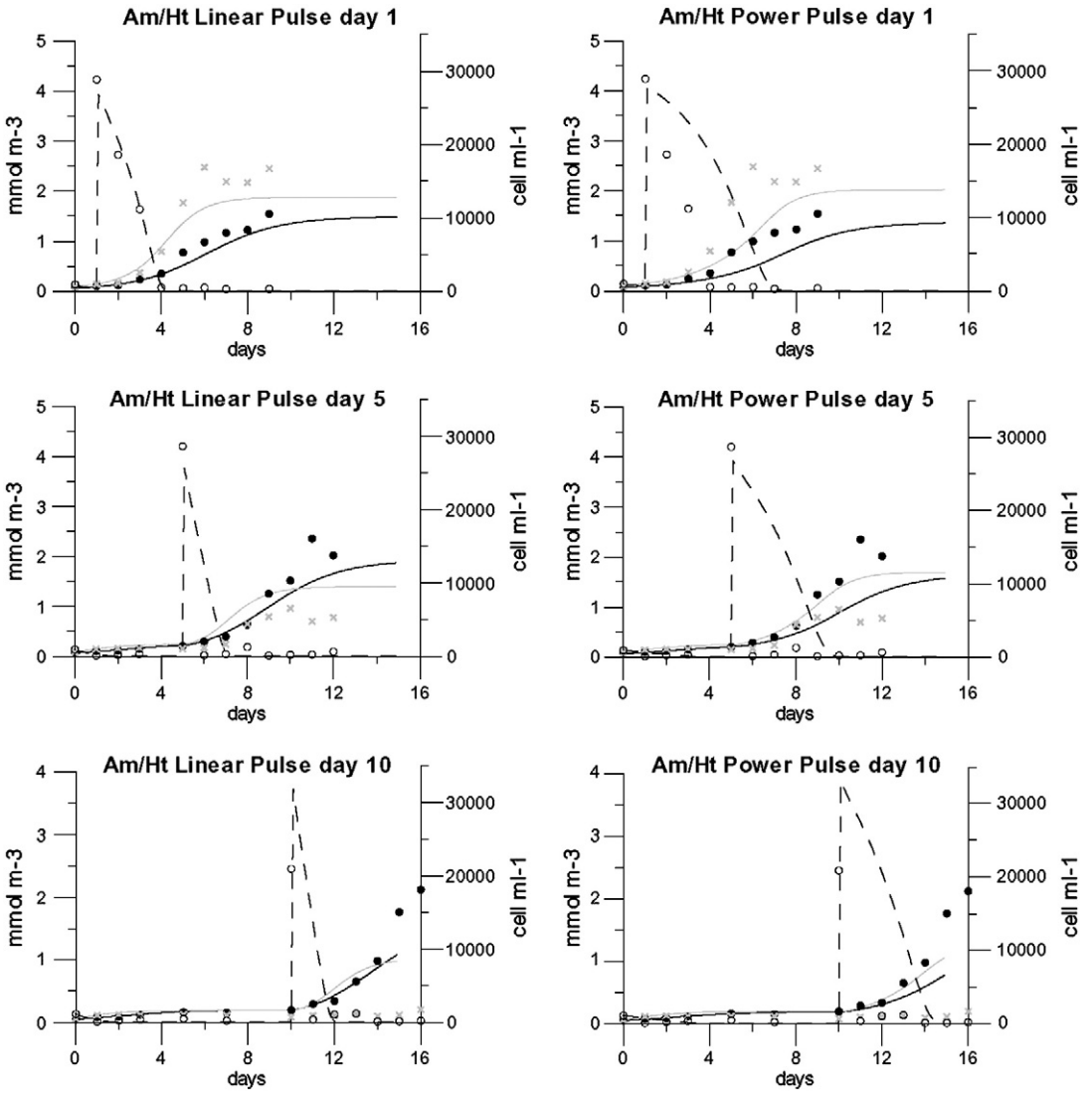

Fig. 7. Simulation of *A. minutum*/*H. triquetra* competition in batch with phosphorus pulse events after 1, 5, and 10 days. –– : *A. minutum* simulation; ●: *A. minutum* data; –– : *H. triquetra* simulation; ×: *H. triquetra* data; — : PO_4 simulation; and O: PO_4 data.

of growth and a linear variation of the maximum uptake linked to phosphorus quota. The model is able to simulate laboratory experiments in semi-continuous culture for both algae. It also enables competition between species to be simulated under different laboratory environments.

In the future we plan to include this model in a more general environmental model. Although this model is capable of simulating the P limited competition between *A. minutum* and *H. triquetra*, the question of how to model other phytoplankton species (diatoms and dinoflagellates) remains. Might it be necessary to model the same complexity for all phytoplankton groups? This would require a large and complex model with a huge amount of data for calibration. Thus, if the primary objective of a model is to describe the risk of a toxic algal bloom, and if, in the case of *A. minutum* in the Penzé estuary, it is not dominant, it may be preferable to simulate it without any feedback on the ecosystem. However, such a model should also evaluate the relevance of other important factors such as physical control (dilution, stratification, etc.), hydrological factors (temperature, light, nutrients, etc.) and plankton dynamics (competition with other phytoplankton species, bacteria, grazing, parasitism, etc.).

Acknowledgements

This research was supported by the Interreg IIB NWE project called Final. We also thank the two referees for their critical appraisal of this work.

References

Aminot, A., Kérouel, R., 2004. Mesures des concentrations en carbone, azote et phosphore organiques particulaires, in: Ifremer (Ed.), Hydrologie des écosystèmes marins. Paramètres et analyses. pp. 194–214.

Aminot, A., Kérouel, R., 2007. Dosage automatique des nutriments dans les eaux marines: méthodes en flux continu. Ed. Ifremer, Méthodes d'analyse en milieu marin. 188 p.

Anderson, D.A., Stock, A.C., Keafer, B.A., Nelson, A.B., Thompson, B., McGillicuddy, D.J., Keller, M., Matrai, P.A., Martin, J., 2005. *Alexandrium fundyense* cyst dynamics in the Gulf of Maine. Deep-Sea Res. II 52, 2522–2542.

Andrieux-Loyer, F., Philippon, X., Bally, G., Kérouel, R., Youenou, A., Le Grand, J., 2008. Phosphorus dynamics and bioavaibility in sediments of the Penzé estuary (NW France) in relation to annual P-fluxes and occurrences of *Alexandrium minutum*. Biogeochemistry 88, 213–231.

Basterretxea, G., Garces, E., Jordi, A., Angles, S., Maso, M., 2007. Modulation of nearshore harmful algal blooms by *in situ* growth rate and water renewal. Mar. Ecol. Prog. Ser. 353, 53–65.

Bechemin, C., Grzebyk, D., Hachame, F., Hummert, C., Maestrini, S.Y., 1999. Effect of different nitrogen/phosphorus nutrient ratios on the toxin content in *Alexandrium minutum*. Aquat. Microb. Ecol. 20, 157–165.

Belin, C., 1993. Distribution of *Dinophysis* spp. and *Alexandrium minutum* along French coasts since 1984 and their DSP and PSP toxicity levels. In: Smayda, T.J., Shimiziu, Y. (Eds.), Toxic Phytoplankton Blooms in the Sea. Elsevier, Amsterdam, pp. 469–474.

Blauw, A.N., Los, F.J., Huisman, J., Peperzak, L., 2010. Prediction of nuisance foam events and *Phaeocystis globosa* blooms in Dutch coastal waters, analyzed with fuzzy logic. Journal of Marine Systems 83, 115–126.

Cembella, A.D., 1998. Ecophysiology and metabolism of paralytic shellfish toxins in marine microalgae. In: Anderson, D.M., Cembella, A.D., Hallegraeff, G.M. (Eds.), Physiological Ecology of Harmful Algal Blooms. Springer-Verlag, Heidelberg, pp. 381–403.

Chapelle A., Andrieux-Loyer F., Fauchot, J., Guillaud, J.F., Labry, C., Sourisseau, M., Verney, R., 2008. Understanding, predicting and tackling algal blooms. "What is the current situation concerning *Alexandrium minutum* in the Penzé estuary?". Rapport Ifremer. 23 p.

Collos, Y., 1983. Transient situations in nitrate assimilation by marine diatom. 4. Non-linear phenomena and the estimation of the maximum uptake. J. Plankton Res. 5 (5), 677–691.

Collos, Y., 1986. Time-lag algal growth dynamics: biological constraints on primary production in aquatic environments. Mr. Ecol. Prog. Ser. 33, 193–206.

Cunnigham, A., Maas, P., 1978. Time lag and nutrient storage effects in the transient growth response of *Chlamydomonas reinhardii* in nitrogen-limited batch and continuous structure. J. Gen. Microbiol. 104 (2), 227–231.

Davidson, K., 1996. Modelling microbial food webs. Mar. Ecol. Prog. Ser. 145, 279–296.

Davidson, K., Cunningham, A., 1996. Accounting for nutrient processing time in mathematical models of phytoplankton. Limnol. Oceanogr. 41 (4), 779–783.

Davidson, K., Gurney, W.S.C., 1999. An investigation of non steady state algal growth. II. Mathematical modelling of co-nutrient limited algal growth. J. Plankton Res. 21, 839–858.

Davison, K., Cunningham, A., Flynn, K.J., 1993. Modelling temporal decoupling between biomass and numbers during the transient nitrogen-limited growth of a marine phytoflagellate. J. Plankton Res. 15, 351–359.

Droop, M.R., 1973. Some thoughts on nutrient limitation in algae. J. Phycol. 9, 264–272.

Ducobu, H., Huisman, J., Jonker, R.R., Mur, L.R., 1998. Competition between a prochlorophyte and a cyanobacterium under various phosphorus regimes: comparison with the Droop model. J. Phycol. 34, 467–476.

Erard-Le Denn, E., 1997. *Alexandrium minutum*. Efflorescences toxiques des eaux côtières françaises. In: Berland, B., Lassus, P. (Eds.), Ecologie, écophysiologie, toxicologie. Repères Océan. 13, pp. 53–66.

Fauchot, J., Saucier, F.J., Levasseur, M., Roy, S., Zakardjian, B., 2008. Wind-driven river plume dynamics and toxic *Alexandrium tamarense* blooms in the St Lawrence estuary (Canada): a modeling study. Harmful algae. 7, 214–227.

Flynn, K.J., 2001. A mechanistic model for describing dynamic multi-nutrient, light, temperature interactions in phytoplankton. J. Plankton Res. 23, 977–997.

Flynn, K.J., 2002. How critical is the the critical N:P ratio? J. Phycol. 38, 961–970.

Flynn, K.J., 2003. Modelling multi-nutrient interactions in phytoplankton, balancing simplicity and realism. Prog. Oceanogr. 56, 249–279.

Flynn, K.J., 2008. Use, abuse, misconceptions and insights from quota models — the Droop cell quota model 40 years on. Oceanogr. Mar. Biol. Annu. Rev. 46, 1–23.

Flynn, K.J., 2010. Ecological modelling in a sea of variable stoichiometry; dysfunctionality and the legacy of Redfield and Monod. Prog. Oceanogr. 84, 52–65.

Flynn, K.J., Page, S., Wood, G., Hipkin, C.R., 1999. Variations in the maximum transport rates for ammonium and nitrate in the prymnesiophyte *Emiliana Huxleyi* and the raphidophyte *Heterosigma carterae*. J. Plankton Res. 21, 355–371.

Geider, R.J., Mac Intyre, H.L., Kana, T.M., 1998. A dynamic regulatory model of phytoplanktonic acclimation to light, nutrients, and temperature. Limnol. Oceanogr. 43, 679–694.

Guillard, R.R.L., Ryther, J.H., 1962. Studies on marine plankton diatoms. I *Cyclotella nana* (Husted) and *Detonela confervacea* (Cleve). Gran. Can. J. Microbiol. 8, 229–239.

Haney, J.D., Jackson, G.A., 1996. Modelling phytoplankton growth rates. J. Plankton Res. 18, 63–85.

Jauzein C., Labry C., Youenou A., Quéré J., Delmas D., Collos Y. Growth and phosphorus uptake by the toxic dinoflagellate *Alexandrium catenella* (Dinophyceae) in response to phosphate limitation. J. Phycol. (in press).

John, E.H., Flynn, K.J., 2000. Modelling phosphate transport and assimilation in microalgae: how much complexity is warranted? Ecol. Model. 125, 145–157.

Labry, C., Herbland, A., Delmas, D., 2002. The role of phosphorus on planktonic production of the Gironde plume waters in the Bay of Biscay. J. Plankton Res. 24, 97–117.

Labry, C., Erard-Le Denn, E., Chapelle, A., Youenou, A., Crassous, M.P., Martin-Jézequel, V., Le Grand, J., 2004. Etude écophysiologique et paramétrisation du rôle du phosphore sur la croissance d'*Alexandrium minutum*, espèce responsable d'eaux colorées toxiques en estuaire de Penzé, et de son principal compétiteur *Heterocapsa triquetra*. Rapport Ifremer PNEC–ART3. 32 p.

Labry, C., Erard-Le Denn, E., Chapelle, A., Fauchot, J., Youenou, A., Crassous, M.P., Le Grand, J., Lorgeoux, B., 2008. Competition for phosphorus between two dinoflagellates: a toxic *Alexandrium minutum* and a non-toxic *Heterocapsa triquetra*. J. Exp. Mar. Biol. Ecol. 358 (2), 124–135.

Maas, E.W., Latter, R.M., Thiele, J., Waite, A.M., Brooks, H.J.L., 2007. Effect of multiple antibiotic treatments on a paralytic shellfish toxin-producing culture of the dinoflagellate *Alexandrium minutum*. Aquat. Microb. Ecol. 48 (3), 255–260.

Maguer, J.F., Wafar, M., Madec, C., Morin, P., Erard-Le Denn, E., 2004. Nitrogen and phosphorus requirements of an *Alexandrium minutum* bloom in the Penze Estuary, France. Limnol. Oceanogr. 49, 1108–1114.

McGillicuddy Jr., D.J., Anderson, D.M., Solow, A.R., Townsend, D.W., 2005. Interannual variability of *Alexandrium fundyense* abundance and shellfish toxicity in the Gulf of Maine. Deep-Sea Res. II 52, 2843–2855.

Mitra, A., Flynn, K.J., 2006. Promotion of harmful algal blooms by zooplankton predatory activity. Biol. Lett. 2, 194–197.

Monod, J., 1942. Recherches sur les croissances des cellules bactériennes. Hermann, Paris. 211 p.

Morel, F.M.N., 1987. Kinetics of nutrient uptake and growth in phytoplankton. J. Phycol. 23, 137–150.

Morin, P. Erard-Le, Denn, E., Maguer, J.F., Madec, C., Videau, C., Le Grand, J., Mace, E., 2000. Etude des causes de proliférations de microalgues toxiques en mer: cas d'*Alexandrium*. Rapport Université Bretagne Occidentale, Ifremer Brest. 135 p.

Nyholm, N., 1978. Dynamics of phosphate limited algal growth: simulation of phosphate shocks. J. Theor. Biol. 70 (4), 415–425.

Probert, I. P., 1999. Sexual reproduction and ecophysiology of the marine dinoflagellate *Alexandrium minutum* Halim. Ph D thesis, University of Westminster, London: 99p.

Riegman, R., Stolte, W., Noordeloos, A.A.M., Slezak, D., 2000. Nutrient uptake and alkaline phosphatase (EC 3:1:3:1) activity of *Emiliana huxleyi* (Prymnesiophyceae) during growth under N and P limitation in continuous cultures. J. Phycol. 36, 87–96.

Roelke, D.L., Eldridge, P.M., Cifuentes, L.A., 1999. A model of phytoplankton competition for limiting and non limiting nutrients: implications for development of estuarine and nearshore management schemes. Estuaries 22, 92–104.

Sciandra, A., 1991. Coupling and uncoupling between nitrate uptake and growth rate in *Prorocentrum minimum* (Dinophyceae) under different frequencies of pulsed nitrate supply. Mar. Ecol. Prog. Ser. 72, 261–269.

Solorzano, L., Sharp, J.H., 1980. Determination of total dissolved phosphorus and particulate phosphorus in natural waters. Limnol. Oceanogr. 25, 754–758.

Thingstad, T.F., 1987. Utilization of P, N, and organic C by heterotrophic bacteria. I. Outline of a chemostat theory with a consistent concept of 'maintenance' metabolism. Mar. Ecol. Prog. Ser. 35, 99–109.

Tilman, D., Kilham, S.S., 1976. Phosphate and silicate growth and uptake kinetics of the diatoms *Asterionella formosa* and *Cyclotella meneghiniana* in batch and semicontinuous culture. J. Phycol. 12, 375–383.

Yamamoto, T., Seike, T., 2003. Modelling the population dynamics of the toxic dinoflagellate *Alexandrium* in Hiroshima Bay. Japan. II. Sensivity to physical and biological parameters. J. Plankton Res. 25, 63–81.

Yamamoto, T., Seike, T., Hashimoto, T., Tarutani, K., 2002. Modelling the population dynamics of the toxic dinoflagellate *Alexandrium tamarense* in Hiroshima Bay (Japan). J. Plankton Res. 24 (1), 33–47.